Front. Phys. China, 2009, 4(3): 269–279
DOI 10.1007/s11467-009-0029-3

REVIEW ARTICLE

Towards graphene nanoribbon-based electronics

Bing HUANG (黄兵), **Qi-min YAN** (严琪闽), **Zuan-yi LI** (李缵轶), **Wen-hui DUAN** (段文晖)(✉)

Department of Physics, Tsinghua University, Beijing 100084, China
E-mail: dwh@phys.tsinghua.edu.cn

Received February 18, 2009; accepted February 23, 2009

The successful fabrication of single layer graphene has greatly stimulated the progress of the research on graphene. In this article, focusing on the basic electronic and transport properties of graphene nanoribbons (GNRs), we review the recent progress of experimental fabrication of GNRs, the theoretical and experimental investigations of physical properties, and device applications of GNRs. We also briefly discuss the research efforts on the spin polarization of GNRs in relation to the edge states.

Keywords graphene nanoribbons, transport, edge disorder, electronic devices, spin polarization

PACS numbers 73.63.-b, 73.22.-f, 71.15.Mb, 83.35.-p

Contents

1 Introduction

Graphene, one monolayer of carbon atoms tightly packed into a two-dimensional honeycomb lattice, is actively being pursued as a material for next-generation electronics due to its promising electronic properties, such as high carrier mobility [1, 2] and long phase coherence lengths [3]. On the other hand, the unique two-dimensional atomic structure of graphene implies unique confinement on electron system and offers a perfect platform to explore the amazing physics phenomenons, such as quantum Hall effect [4–7] and massless Dirac fermions [7–12].

The first task for experimentalists in studying graphene electronics is to fabricate high-quality single layer graphene. Until now, several different experimental methods have been proposed and realized to prepare single layer (or few layers) graphene, including mechanical exfoliation of highly oriented pyrolytic graphite [1], patterned epitaxially grown graphene on silicon carbide or transition metal (e.g., Ru, Ni) substrates [2, 13–15], liquid-phase exfoliation of graphite [16–18], substrate-free gas-phase synthesis [19], and chemical vapor deposition [20, 21]. The success in fabricating single layer graphene has stimulated the extensive research efforts (both theoretical and experimental) in graphene related research area.

The ultimate goal of the use of graphene in next-generation electronics is to realize all-graphene circuits with functional devices built from graphene layers or graphene nanoribbons (GNRs) [22, 23]. As the basic building blocks of such circuit, the concept of electronic devices based on graphene have been proposed theoretically and have been realized recently by experiments. Examples of such are field effect transistors [23–26], P–N junctions [27–30], gas molecule sensor [31–33], and so on.

In this article, we will focus our discussion on the basic electronic and transport properties of GNRs and their application to electronic devices. In particular, the theoretical investigations of GNRs physics and the technical aspects of GNR-based electronic devices will be reviewed in detail. For other topics on the recent experimental and theoretical research efforts on graphene, please refer to the reviews by Katsnelson [34], Geim *et al.* [35], Beenakker [36], and Castro Neto *et al.* [37].

2 Experimental fabrication of graphene nanoribbons

The realization of graphene electronics relies on the

ability to modify the electronic properties of finite-size graphenes (for example, from semiconducting to metallic) by varying their size, shape, and edge orientation. Such a unique property compared to traditional semiconductor materials, such as silicon, would ultimately enable the design and miniaturization of future electronic circuit by patterned graphene. One of the most important issues in patterned graphene fabrication is the control of the nanoribbon width. In order to take advantage of quantum confinement effects in graphene, the ribbon width should go down to the nanometer scale. To realize the patterning of graphene with nano scale width, several different techniques have been proposed including standard e-beam lithography [Fig. 1(a)] [38, 39], microscope lithography [Fig. 1(b)] [40–42], chemical method [Fig. 1(c)] [43], metallic nanoparticle etching [44], and e-beam irradiation of ultrathin poly(methylmethacrylate) (PMMA) [45]. As shown in Fig. 1(a), the scanning electron microscopy (SEM) image reveals that the graphene can be patterned by traditional e-beam lithography technique into nanoribbons with various widths ranging from 20 to 500 nm [39]. Figure 1b shows 10-nm-wide nanoribbon etched via scanning tunnelling microscope (STM) lithography. By setting the optimal lithographic parameters, it is possible to cut GNRs with suitably regular edges, which constitutes a great advancement toward the reproducibility of GNR-based devices [40]. Figure 1c shows atomic force microscopy images of chemically derived GNRs with various widths ranging from 50 nm to sub-10 nm. These GNRs have atomic-scale ultrasmooth edges [43].

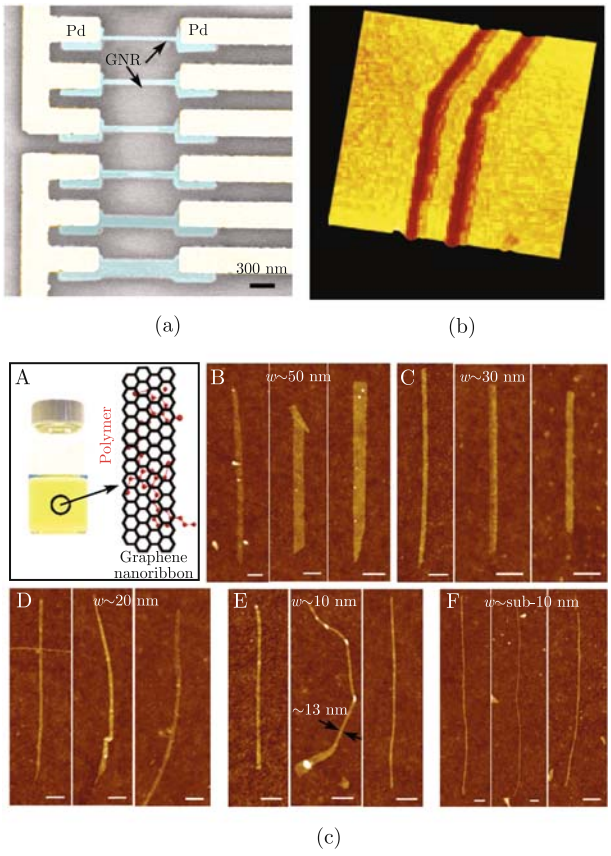

Fig. 1 Various GNRs got from different experimental methods. **(a)** The SEM image of GNRs patterned by e-beam lithography. Reprinted with permission from Ref. [39]. Copyright © 2007 Elsevier. **(b)** An 8-nm-wide 30° GNR bent junction connecting an armchair and a zigzag nanoribbon etched by STM lithography. Reprinted with permission from Ref. [40]. Copyright © 2008 Nature Publishing Group. **(c)** GNRs are got by using simple chemical methods. Reprinted with permission from Ref. [43]. Copyright © 2008 American Association for the Advancement of Science.

The electronic properties of GNRs exhibit a strong dependence on the orientation of their edges. As two typical types of GNRs, armchair GNRs (AGNRs) and zigzag GNRs (ZGNRs) can be obtained by lithography technology along the specific orientation on graphene [Fig. 2(b)] [38, 40]. Actually, the detailed edge structures (both armchair and zigzag) have already been clearly observed in recent experiments [46–48]. One of the most serious obstacle to graphene electronic application is the reliable control of the edge structure of GNRs. Theoretical studies predict that edge states (in a manner similar to the well-known concept of surface states of a 3D crystal) in graphene are strongly dependent on the edge termination and affect the physical properties of GNRs [23, 49–54]. However, until now, there is no reliable experimental method that is able to exactly control the edge structures and reduce their roughness. An interesting experimental observation is that the band gaps of GNRs show little orientation dependence [38], and all fabricated GNRs show semiconducting behavior [55], that seems inconsistent with theoretical results [49–51]. One of the reasons for such inconsistency comes from the roughness of GNR edges, and our explanation is also given in the following part of the article. Another issue related to GNR edges is edge passivation. Since the dangling bonds from the edge carbon atoms have relatively high chemical activity, there is the possibility that other chemical elements present in the material fabrication process (such as C, O, N, H, and other chemical groups formed by these atoms) would interact with the edge atoms and modify the electronic properties of GNRs. To the best of our knowledge, this issue has not been properly solved experimentally.

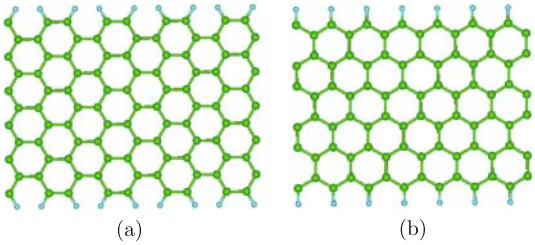

Fig. 2 The structures of H-passivated 11-AGNR **(a)** and 6-ZGNR **(b)**, where big green balls and small blue balls represent carbon atoms and hydrogen atoms, respectively. Integer N is their width index.

3 Elementary electronic and transport properties of graphene nanoribbons

Next, we will review some basic electronic and transport properties of GNRs from the theoretical viewpoint. Figure 2(a) and (b) show two typical models of armchair and zigzag GNRs in first principles or other atomic-level electronic structure calculations, noted as 11-AGNR and 6-ZGNR, respectively. Here, the numbers 11 and 6 are defined as the width index, N. In order to remove the effect of dangling bonds, the edges of GNRs are saturated by hydrogen atoms. As geometrically terminated graphene, the electronic structure of GNRs can be modelled by imposing appropriate boundary conditions on Schrödinger's equation with simple tight-binding (TB) approximations based on π-states of carbon [49, 50]. Another way to get the band structure is to solve two-dimensional Dirac's equation of massless free particles with an effective speed of light to model GNR system [56]. Within these models, it is predicted that GNRs with armchair-shaped edges can be either metallic or semiconducting depending on their widths, as shown in Fig. 3(a). On the other hand, the GNRs with zigzag-shaped edges are metallic with peculiar edge states on both sides of ribbons regardless of their widths, as shown in Fig. 4(a) [49, 50, 57].

Further detailed *ab initio* and GW quasiparticle calculations show that all of the AGNRs exhibit semiconducting behavior, and the energy gaps decrease as a function of increasing ribbon widths. The variation in energy gaps can be separated into three distinct family behaviors [23, 52, 53, 58], as shown in Fig. 3(b). As mentioned above, such dependence of band gap on the geometrical structure of GNR offers a unique possibility to modify

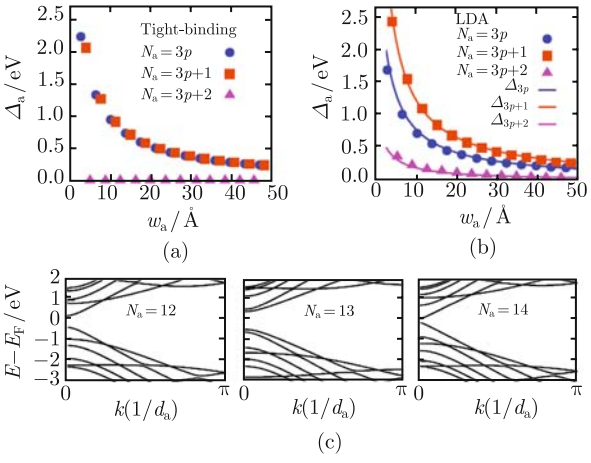

Fig. 3 The variation of band gaps of N_a-AGNRs as a function of width (w_a) obtained **(a)** from TB calculations and **(b)** from first-principles calculations (symbols). **(c)** First-principles band structures of N_a-AGNRs with N_a= 12, 13, and 14, respectively. Reprinted with permission from Ref. [52]. Copyright © 2006 American Physical Society.

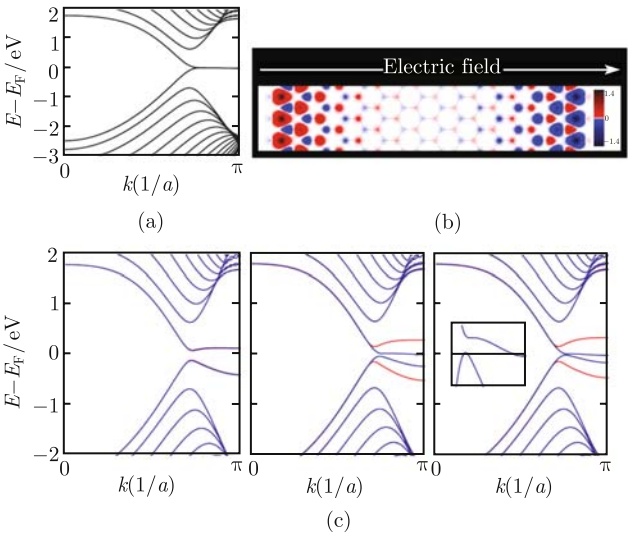

Fig. 4 Electronic structures of graphene nanoribbons. In all figures, the Fermi energy (E_F) is set to zero. **(a)** The spin-unpolarized band structure of a 16-ZGNR. **(b)** The spatial distribution of the charge difference between α-spin and β-spin for the ground state when there is no external field. The magnetization per edge atom for each spin on each sublattice is $0.43\mu_B$ with opposite orientation, where μ_B is the Bohr magneton. The graph is the electron density integrated in the z direction, and the scale bar is in units of 10^{-2}eÅ^{-2}. **(c)** From left to right, the spin-resolved band structures of a 16-ZGNR with the external field of 0.0, 0.05, and 0.1 V/Å, respectively. The red and blue lines denote bands of α-spin and β-spin states, respectively. Reprinted with permission from Ref. [57]. Copyright © 2006 Nature Publishing Group.

the electronic properties of GNRs simply by controlling the width and edge orientation in order to realize all-graphene functional devices.

Upon inclusion of the spin degrees of freedom within the density functional theory (DFT) calculations, ZGNRs are predicted to have a magnetic insulating ground state with ferromagnetic ordering at each zigzag edge and antiparallel spin orientation between the two edges [52, 57], as shown in Fig. 4(b). The spin polarization originates from the edge states that introduce a high density of state (DOS) at the Fermi energy. It can be qualitatively understood in terms of the Stoner magnetism of *sp* electrons (in analogy to conventional *d* electrons), which occupy a very narrow edge band and render instability of spin-band splitting [59]. What is more interesting is that, the zigzag GNRs show half-metallic behavior when external transverse electric field is applied across the ZGNRs along the lateral direction [57], as shown in Fig. 4(c). However, such spin related half-metallic phenomenon becomes weak with an increasing ribbon width (since the total energy difference per edge atom between spin-unpolarized and spin-polarized edge states is only about 20 meV in their simulation system and decreases with increasing width) and is not energetically stable if the width of GNR is significantly larger than the decay length of the spin-polarized edge states [60, 61]. On the other hand, it is predicted that the

half-metallicity can be also achieved in edge-modified or doped ZGNRs [62–65].

Another important issue regarding the basic electronic structures of GNRs relies on edge states. Due to the presence of edge states, the π and π^* subbands of metallic ZGNRs (in the spin-unpolarized state) do not cross with each other at the Fermi level to span the whole energy range like metallic armchair carbon nanotubes (CNTs) [the left panel of Fig. 5(a)]. This leads to the fact that the transport property of ZGNRs under a low bias voltage (or a small potential step) is only determined by the transmission between π and π^* subbands [as shown in Fig. 5(a)]. With the presence of such unique band structures, ZGNRs exhibit two distinct transport behaviors depending on the existence of σ mirror symmetry with respect to the midplane between two edges [66–69], although all the ZGNRs have similar metallic energy band structures. Since the π and π^* subbands of symmetric ZGNRs (i.e., width index N is an even number) have opposite definite σ parities, the transmission between them is forbidden [the left panel of Fig. 5(b)]. However, for asymmetric ZGNRs (i.e., width index N is an odd number), their π and π^* subbands do not have definite σ parities, so the coupling between them can contribute to about one conductance quantum [the right panel of Fig. 5(b)]. This transport difference can be clearly reflected in the current-bias-voltage (I–$V_{\rm bias}$) characteristics of ZGNRs by using the first-principle transport simulation, as shown in Fig. 5(c). Although metallic armchair carbon nanotubes also have π and π^* subbands with definite parities, such symmetry-depending (or band-selective) I–$V_{\rm bias}$ characteristics cannot be observed in them because of the crossover of their subbands, i.e., the absence of edge states. Recently, theoretical work predicts a very large magnetoresistance in a graphene nanoribbon device due to the existence of edge states [70].

Besides the fabrication and theoretical study of monolayer graphene and GNRs, recent experimental [71–73] and theoretical [74–77] studies are also carried out on

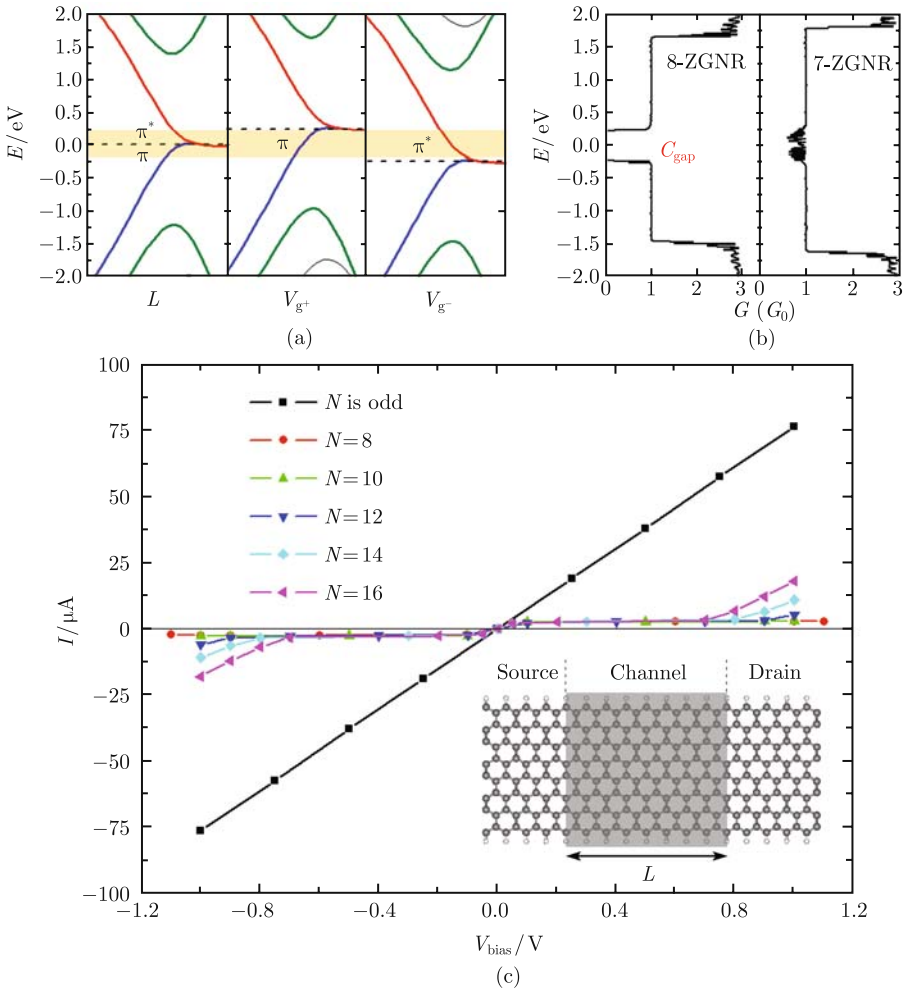

Fig. 5 **(a)** Schematic band structure around the Fermi level of a ZGNR under a positive (V_g+) and a negative (V_g−) potential step. **(b)** Conductance of 8-ZGNR and 7-ZGNR under two potential steps shown in **(a)**. **(c)** I–$V_{\rm bias}$ curves of the two-probe system (see the inset) made of ZGNRs with different widths N. Reprinted with permission from Ref. [66].

bilayer graphene and GNRs. Theoretically, it is shown that the bilayer GNRs and monolayer GNRs have some similar electronic properties such as edge states localized at the zigzag edges and semiconducting behavior of armchair bilayer GNRs [75–77]. Experimentally, it was found that the bilayer graphene has unique features such as anomalous integer quantum Hall effects [71], which is absent in single layer graphene. Moreover, the size of energy gap of such bilayer structures can be controlled by adjusting the carrier concentration [72] as well as by an external electric field [73]. These unique properties open an opportunity to implement bilayer graphene or GNRs in various electronic applications.

4 Edge disorder in graphene nanoribbons

As mentioned above, current experimental techniques (such as lithography) are not able to realize exact control of the edge structures of GNRs, and the edges are always very rough due to the limitation of the fabrication technology [38, 39]. There are theoretical evidences that such edge disorders can significantly change the electronic properties of GNRs [78–83], and lead to some unexpected physics effect, such as the Anderson localization [84, 85] and Coulomb blockade effect [86]. These effects have already been observed in lithographically obtained graphene nanoribbons [29, 38, 87–89].

The edge roughness is also crucial for the spin polarized properties of GNRs. As we know, the magnetic properties of GNRs depend on the highly degenerate edge states. In principle, a perfect edge structure is necessary for stabilizing magnetic properties of GNRs as theoretically predicted. An important question is, how robust the spin-polarized state is in the presence of edge defects and impurities? The answer to this question is not only scientifically interesting to better understand the physical mechanism of spin polarization in GNRs but also has important technological implications in the reliability of GNRs as a new class of spintronic materials. First-principles theoretical studies reveals the effect of edge vacancies and substitutionally doped boron atoms, as typical examples of structural edge defects and impurities, on the spin-polarization of ZGNRs [59]. The calculated energy difference between the magnetic state [both antiferromagnetic (AF) and ferromagnetic (FM)] and the nonmagnetic state is found to rapidly decrease with increasing defect concentration and eventually decrease to zero (nonmagnetic), as shown in Fig. 6. The critical defect (impurity) concentration is found to be $\sim 0.10/\text{Å}$ when the ribbon width is larger than 2 nm.

Evidently, the magnetism in GNRs depends on a high density of state (DOS) around the Fermi energy coming from the highly degenerate edge states in a perfect ribbon edge (E_F) that renders instability of spin polarization [59]. The presence of edge vacancies and impurities would decrease the DOS at E_F since they do not contribute to the same edge state. From the Stoner model, such decrease of DOS will suppress the spin polarization of GNR systems. Therefore, the practical realization of the spin polarization in GNRs for spintronics applications could be rather challenging [59]. Recently, an interesting theoretical work systematically studied the spin current in rough GNRs and predicted that only GNRs with imperfect edges exhibit a nonzero spin conductance while there is no spin current in perfect GNRs [90]. It confirms that the edge effect is of great importance to spin-related properties of GNRs.

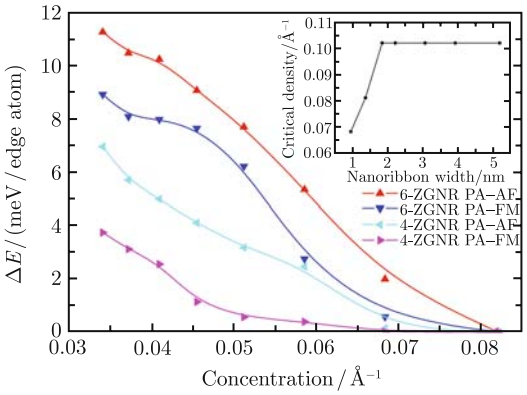

Fig. 6 The energy difference per edge atom between the magnetic (AF or FM) and paramagnetic (PA) state as a function of vacancy concentration in the edge. Two different ribbon widths of N=6 and N=4 are shown. The inset shows the critical concentration as a function of the ribbon width up to 5 nm. Reprinted with permission from Ref. [59]. Copyright © 2008 American Physical Society.

Furthermore, the problem of edge passivation has not yet been clearly resolved experimentally until now. From the theoretical viewpoint, the edge passivation can be well modeled by the modifications of the hopping energies in the tight-binding approach [91] or via additional phases in the boundary conditions [92]. Recent theoretical modeling and calculations have indicated that the edge passivation has a strong effect on the electronic and spin-polarized properties of GNRs [62–64]. The possible passivation species include hydrogen, carbon, oxygen, nitrogen, and other chemical groups. Further experimental works are needed to explore the realistic edge structures of GNRs at atomic scale and determine which types of edge passivation are favorable.

5 Transistors based on graphene nanoribbons

The interesting and unique electronic properties of GNRs, such as orientation and width dependence of transport behavior, offer great possibilities for their electronic device applications. Compared with other electronic materials, one of the most promising advantage

of GNRs is that GNR-based devices and even integrated circuits can be fabricated by a single process of patterning a graphene sheet [23]. Figure 7(a)–(c) illustrate three basic device building blocks: (i) metal-semiconductor junction, (ii) P–N junction, and (iii) hetero-junction, which can be, respectively, made by patterned GNRs (i) along different direction, (ii) with different edge doping, and (iii) with different widths. It was proposed that a variety of devices can be constructed from these building blocks. For example, a field effect transistor (FET) can be made simply by two metal-semiconductor junctions, as shown in Fig. 7(d). There are some potential key advantages in designing and constructing device architectures based on GNRs. The first advantage is the perfect atomic interface, a feature that is difficult to achieve for the interconnection between nanotubes of different diameter and chirality. Second, it is generally difficult to find a robust method to make contact with the molecular device unit, because there usually exists a large contact resistance between the metal electrodes and molecules (e.g., single-walled CNT) due to a very small contact area. This difficulty may be circumvented by using GNRs, because the GNR-based devices can be connected to the outside circuits exclusively via metallic GNRs (or graphene), as illustrated in Fig. 7(d), which serve as extensions of metal electrodes to make contact with the semiconducting GNRs so that an atomically smooth metal-semiconductor interface is maintained with minimum contact resistance. Last but not the least, the edges of GNRs may serve as effective sites for doping. In principle, by introducing different types of dopants at different sections of GNR edges, one can realize a P–N junction by selective doping, as shown in Fig. 7(b).

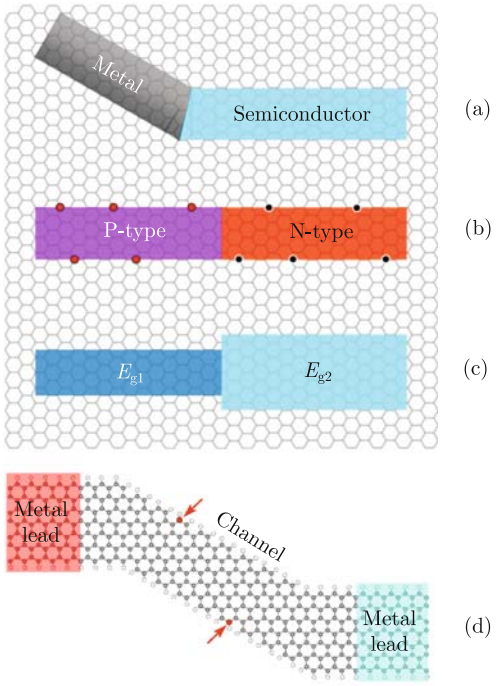

Fig. 7 Schematics of three device building blocks: **(a)** a metal-semiconductor junction between a zigzag and an armchair GNR. **(b)** a P–N junction between two armchair GNRs with different edge doping, and **(c)** a heterojunction between two armchair GNRs of different widths (band gaps). **(d)** Schematics of a GNR–FET, which is made from one semiconducting 10-AGNR channel and two metallic 7-ZGNR leads connected to two external metal electrodes. Reprinted with permission from Ref. [23]. Copyright © 2007 American Chemical Society.

One of the most important electronic applications based on GNRs is field effect transistors. Recently, experimental studies [38, 39, 43, 55] have indicated the possibility of fabricating GNR-based transistors. The advantage of GNRs as an alternative material for transistors is that it could bypass the chirality challenge of CNTs while retaining the excellent electronic properties of graphene sheets, such as the high I_{on}/I_{off} ratio and excellent electron/hole mobilities. The performance of one sub-10-nm GNR–FET in the latest work from Dai's group is shown in Fig. 8(a) and (b) (the transfer and output characteristics, respectively, for the GNR device with the width of $\sim 2 \pm 0.5$ nm and the channel length of $\sim$ 236 nm) [55]. This device delivered $I_{on} \sim 4$ μA at $V_{ds} = 1$ V, I_{on}/I_{off} ratio $> 10^6$ at $V_{ds} = 0.5$ V, subthreshold slope S=dV_{gate}/dlg $I \sim 210$ mV/decade and transconductance ~ 1.8 μS (∼900 μS/μm). The device performance is comparable with the best CNT-based transistors. However, the Dirac point was not observed around zero gate bias in this measurement, indicating p-doping effects at the edges or by physisorbed species during the chemical treatment steps.

Together with experimental progress on GNR-based transistors, theoretical studies using semiclassical and quantum transport models show that GNR-based FETs could have a similar performance as CNT-based FETs and might outperform traditional Si-based FETs [23, 93–95]. Figure 9 shows a first-principles study on the performance of a typical GNR-based FET made with a 5.91-nm long intrinsic semiconducting 10-AGNR channel connected to two metallic 7-ZGNR leads (source and drain) [23]. In Fig. 9(a), the near-symmetric I–V_{gate} curve shows an excellent ambipolar transistor with ON/OFF ratio $I_{on}/I_{off} \sim 2000$ and subthreshold swing of $S \sim$ 60 mV/decade, which are comparable to those of high-performance CNT–FETs. Such field effect can be clearly reflected in the change of I–V_{bias} characteristics under different gate voltages [Fig. 9(b)]. Figure 9(c) shows the I–V_{gate} curves of the GNR–FETs made from the same 10-AGNR channel with its length ranging from 1.69 to 6.76 nm, from which the values of S are derived as a function of L, as shown in Fig. 9(d). Clearly, S decreases with increasing L and gradually approaches ∼60 mV/decade when L becomes longer than 6 nm. Meanwhile, the ON-current stays the same, independent of

L, but the OFF-state leakage current increases rapidly with decreasing L, which gives rise to a large S. The performance of the ambipolar GNR–FETs made of intrinsic semiconductor channels can be understood in terms of metal-semiconductor tunneling junctionh within the semiclassical band-bending model.

Compared with the basic ambipolar FETs, it is well known that N-type (or P-type) FETs serve as critical transistor devices for digital electronics applications [96, 97]. To realize such device design based on GNRs, a method was proposed using N (or B) atoms as selective dopants at the channel region of perfect GNR–FETs [the positions of B or N are indicated by arrows in Fig. 7(d)]. Figure 9(e) and (f) shows the calculated I–$V_{\rm gate}$ curves under $V_{\rm bias} = 20$ mV, exhibiting the typical behavior of a N-type P-type) FET [23]. It is suggested that all of the functional transistor devices that work in traditional Si-based circuits could be realized by GNRs and GNR-based junctions in principle.

Noting the current experimental difficulty to get an accurate Z-shape junction [i.e., FET shown in Fig. 7(d)] due to the limitation of lithography technique, a new type of field effect transistor has also been proposed, taking advantage of the metal-semiconductor transition in ZGNRs induced by substitutional doping of nitrogen or boron atoms at their edges [98], as shown in Fig. 10(a). Besides simplifying the fabrication process, such linear configuration can also increase the device density in electronic circuits. Figure 10(b) shows a typical I-$V_{\rm gate}$ curve for the N-doped GNR–FET (with the channel length of 8.54 nm) under the bias voltage $V_{\rm bias} = 0.01$ V. Clearly, the doped FET exhibits ambipolar characteristics, similar to the Z-shape FETs. The relationship between the device performance and the channel length is demonstrated by calculating I–$V_{\rm gate}$ curve of N-doped GNR–FETs as a function of the doped channel length while keeping the bias voltage $V_{\rm bias}$ at 0.01 V. As shown in Fig. 10(c), the subthreshold swing S of these doped GNR–FETs decreases, and the ON/OFF current ratio increases exponentially. It can be seen that for good device performance with small S value (e.g., below 100 mV/decade) and high ON/OFF current ratio (e.g., above 100), the doped channel length should be longer than 5 nm. The minimum leakage current of those FETs with the doped channels shorter than this critical length will be greatly enhanced by direct tunneling, which lowers the device performance.

Besides ideal case, some more practice issues concern

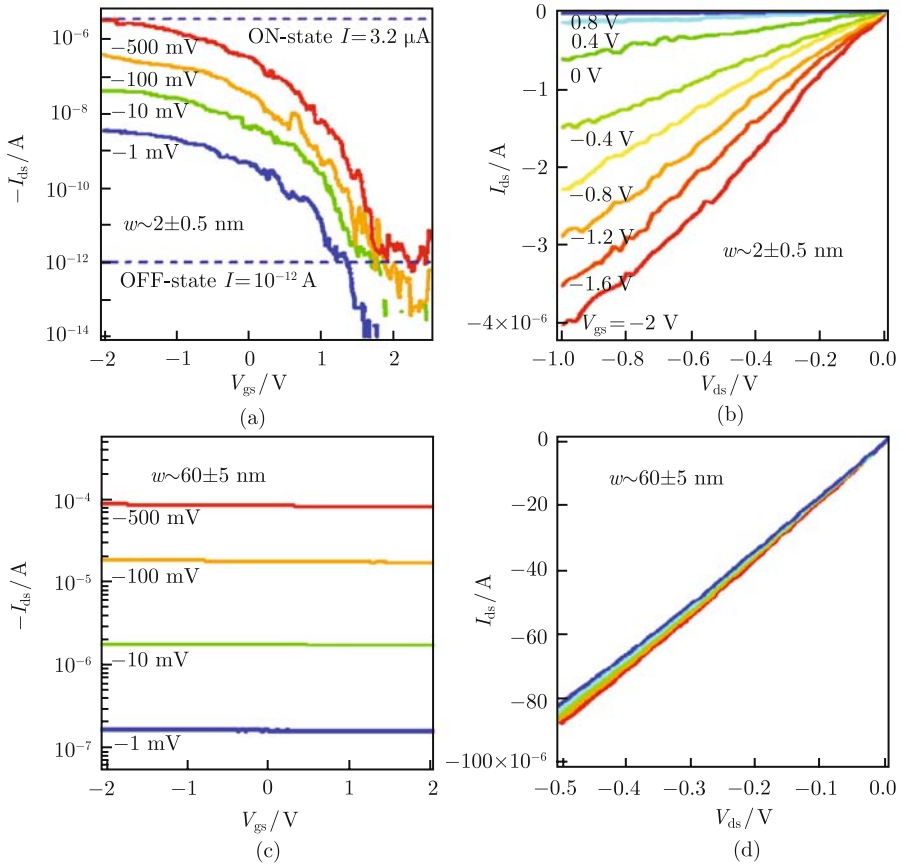

Fig. 8 **(a)** and **(b)** Transistor performance of GNR–FETs with width of ∼ 2 nm and channel length of ∼ 236 nm [**(c)** and **(d)**, width of ∼ 60 nm, and channel length of ∼ 190 nm]. **(a)** Transfer characteristics (current vs. gate voltage $I_{\rm ds}$–$V_{\rm gs}$) under various $V_{\rm ds}$. $I_{\rm ON}/I_{\rm OFF}$ ratio of $> 10^6$ is achieved at room temperature. **(b)** Output characteristics ($I_{\rm ds}$–$V_{\rm ds}$) under various $V_{\rm gs}$. On current density is ∼ 2000 μA/μm in this device. **(c)** Transfer and **(d)** output characteristics of the 60-nm width GNR–FET device. Reprinted with permission from Ref. [55].

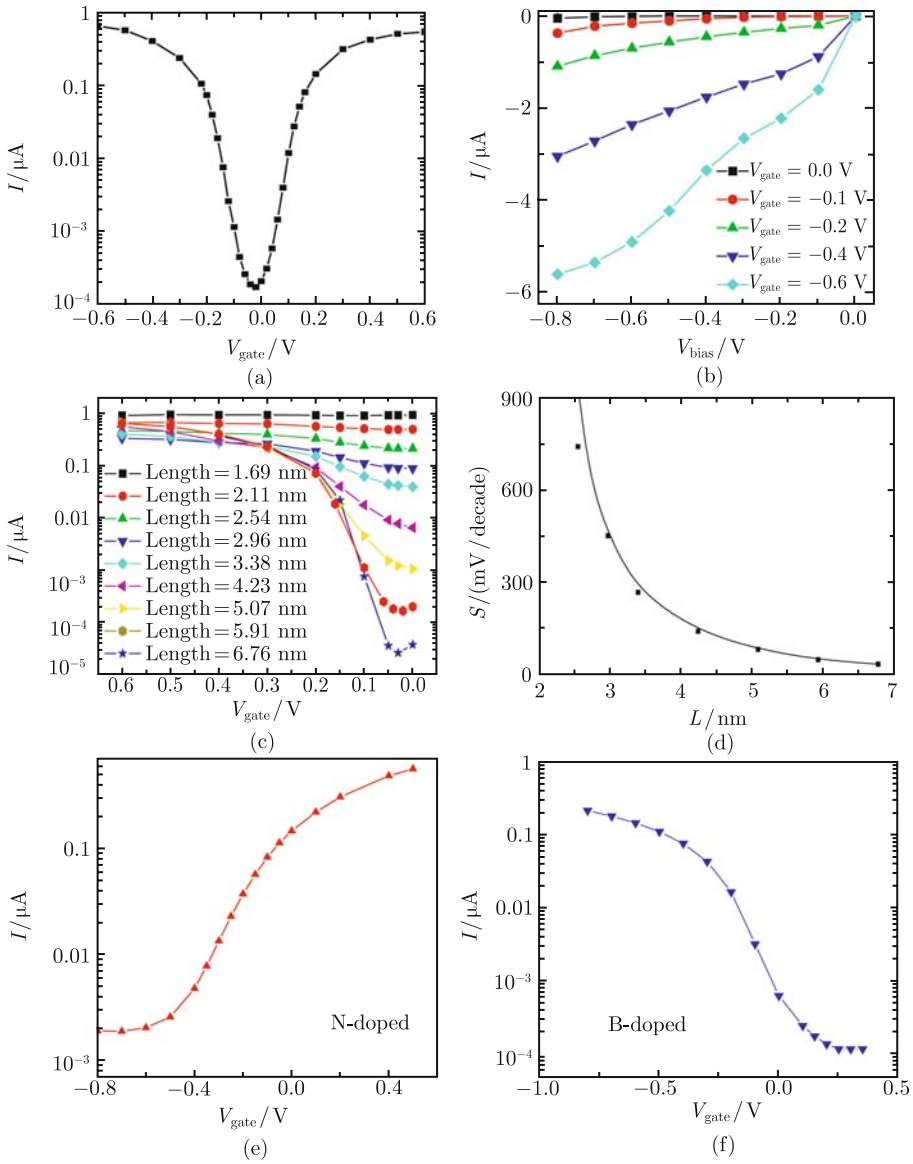

Fig. 9 **(a)** I–$V_{\rm gate}$ curve for a 5.91-nm long intrinsic 10-AGNR channel ($V_{\rm bias}$=20 mV). **(b)** I–$V_{\rm bias}$ curves under different gate voltage ($V_{\rm gate}$). **(c)** I–$V_{\rm gate}$ curves for different channel lengths ($V_{\rm bias}$=20 mV). **(d)** The subthreshold swing (S) as a function of channel length L. **(e)**, **(f)** I–$V_{\rm gate}$ curves for a 5.91 nm long 10-AGNR channel with selective N and B doping, respectively ($V_{\rm bias}$=20 mV). Reprinted with permission from Ref. [23]. Copyright © 2007 American Chemical Society.

-ing GNR-based FETs are discussed in recent theoretical works. For example, the effects of the various contact types and shapes on the performance of Schottky-barrier-type GNR–FETs have been investigated theoretically [99], which indicates that the semi-infinite normal metal can potentially provide promising performance. In addition, the effect of edge roughness and carrier scattering on GNR–FETs have been studied [100–102]. The presence of edge disorder significantly reduces ON-state currents and increases OFF-state currents (the ON/OFF ratio decreases), and introduces wide variability across devices. These effects become weaker for GNRs with larger width and smoother edges. However, the band gap decreases with increasing width, thereby increasing the band-to-band tunneling mediated subthreshold leakage current even with perfect GNRs. Obviously, without atomically precise edge control during fabrication, it is hard to get reliable and stable performance of GNR–FETs.

Due to their unusual basic properties, GNRs as well as graphene are promising for a large number of applications [35, 83], from spin filters [63, 90, 103], valley filters [104], to chemical sensors [31, 33, 105]. GNRs can be chemically and/or structurally modified in order to change its functionality and hence its potential applications.

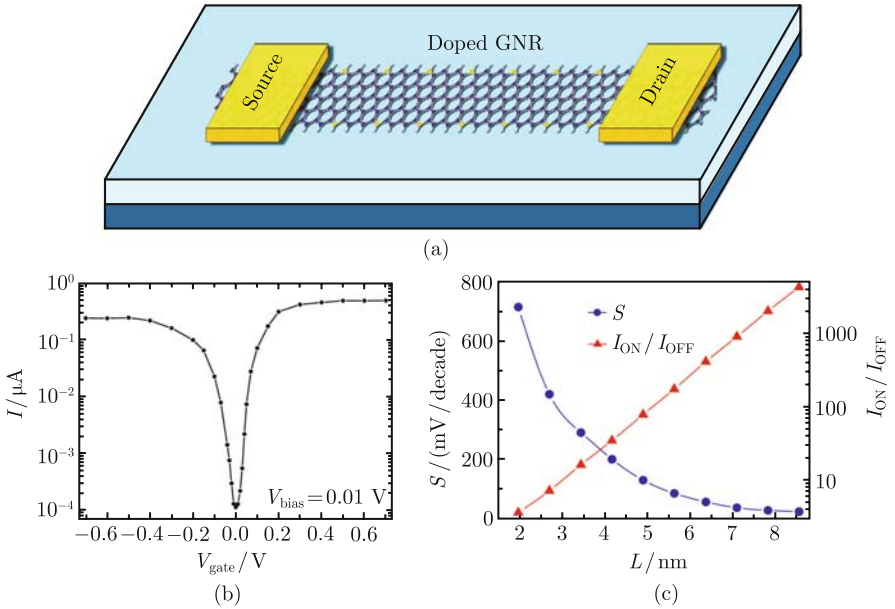

Fig. 10 **(a)** The schematic structure of the field effect transistor (FET) made from a single 5-ZGNR. The semiconducting channel is obtained by edge doping of N in a finite-length region (*the center region*). **(b)** Simulated I–V_{gate} curves of N-doped GNR–FETs under V_{bias} = 0.01 V. The channel length is 8.54 nm, and the linear doping concentration is 0.1365 Å^{-1}. **(c)** The dependence of the subthreshold swing S (*blue line*) and the ON/OFF current ratio (*red line*) on the channel length L. Reprinted with permission from Ref. [98]. Copyright © 2007 American Institute of Physics.

6 Summary

In summary, we reviewed the basic electronic and transport properties of graphene nanoribbons, and discussed recent theoretical and experimental progress on GNR-based field effect transistors from the viewpoint of device application. Due to the interesting electronic and magnetic properties, GNRs have been demonstrated as a promising candidate material for future post-silicon electronics such as transport materials, field effect transistors, and spin injection or filter. More experimental efforts will focus on fabricating high-quality nanoribbon samples with accurate control of the edge structures.

Acknowledgements This work was supported by the Ministry of Science and Technology of China (Grant Nos. 2006CB605105 and 2006CB0L0601), and the National Natural Science Foundation of China.

References

1. K. S. Novoselov, A. K. Geim, S. V. Morozov, D. Jiang, Y. Zhang, S. V. Dubonos, I. V. Grigorieva, and A. A. Firsov, Science, 2004, 306: 666
2. C. Berger, Z. Song, T. Li, X. Li, A. Y. Ogbazghi, R. Feng, Z. Dai, A. N. Marchenkov, E. H. Conrad, P. N. First, and W. A. de Heer, J. Phys. Chem. B, 2004, 108: 19912
3. C. Berger, Z. Song, X. Li, X. Wu, N. Brown, C. Naud, D. Mayou, T. Li, J. Hass, A. N. Marchenkov, E. H. Conrad, P. N. First, and W. A. de Heer, Science, 2006, 312: 1191
4. V. P. Gusynin and S. G. Sharapov, Phys. Rev. Lett., 2005, 95: 146801
5. K. S. Novoselov, Z. Jiang, Y. Zhang, S. V. Morozov, H. L. Stormer, U. Zeitler, J. C. Maan, G. S. Boebinger, P. Kim, and A. K. Geim, Science, 2007, 315: 1379
6. Y. Zhang, Y. W. Tan, H. L. Stormer, and P. Kim, Nature (London), 2005, 438: 201
7. K. S. Novoselov, A. K. Geim, S. V. Morozov, D. Jiang, M. I. Katsnelson, I. V. Grigorieva, S. V. Dubonos, and A. A. Firsov, Nature (London), 2005, 438: 197
8. S. Y. Zhou, G. H. Gweon, J. Graf, A. V. Fedorov, C. D. Spataru, R. D. Diehl, Y. Kopelevich, D. H. Lee, S. G. Louie, and A. Lanzara, Nature Phys., 2006, 2: 595
9. A. Bostwick, T. Ohta, T. Seyller, K. Horn, and E. Rotenberg, Nature Phys., 2007, 3: 36
10. G. Li and E. Y. Andrei, Nature Phys., 2007, 3: 623
11. C. H. Park, L. Yang, Y. W. Son, M. L. Cohen, and S. G. Louie, Nature Phys., 2008, 4: 213
12. Z. Q. Li, E. A. Henriksen, Z. Jiang, Z. Hao, M. C. Martin, P. Kim, H. L. Stormer, and D. N. Basov, Nature Phys., 2008, 4: 532
13. D. Usachov, A. M. Dobrotvorskii, A. Varykhalov, O. Rader, W. Gudat, A. M. Shikin, and V. K. Adamchuk, Phys. Rev. B, 2008, 78: 085403
14. P. W. Sutter, J. Flege, and E. A. Sutter, Nature Mater., 2008, 7: 406
15. D. Martoccia, P. R. Willmott, T. Brugger, M. Bjorck, S. Gunther, C. M. Schleputz, A. Cervellino, S. A. Pauli, B. D. Patterson, S. Marchini, J. Wintterlin, W. Moritz, and T. Greber, Phys. Rev. Lett., 2008, 101: 126102
16. Y. Hernandez, V. Nicolosi, M. Lotya,F. M. Blighe, Z. Sun, S. De, I. T. McGovern, B. Holland, M. Byrne, Y. K. Gunko, J. J. Boland, P. Niraj, G. Duesberg, S. Krishnamurthy, R. Goodhue, J. Hutchison, V. Scardaci, A. C. Ferrari, and J. N. Coleman, Nature Nanotechnology, 2008, 3: 563

17. X. Fan, W. Peng, Y. Li, X. Li, S. Wang, G. Zhang, and F. Zhang, Adv. Mater., 2008, 20: 4490
18. V. C. Tung, M. J. Allen, Y. Yang, and R. B. Kaner, Nat. Nanotechnol., 2009, 4: 25
19. A. Dato, V. Radmilovic, Z. Lee, J. Phillips, and M. Frenklach, Nano Lett., 2008, 8: 2012
20. A. Reina, X. Jia, J. Ho, D. Nezich, H. Son, V. Bulovic, M. S. Dresselhaus, and J. Kong, Nano Lett., 2009, 9: 30
21. K. S. Kim, Y. Zhao, H. Jang, S. Y. Lee, J. M. Kim, K. S. Kim, J. H. Ahn, P. Kim, J. Y. Choi, and B. H. Hong, Nature (London), 2009, 457: 706
22. D. A. Areshkin and C. T. White, Nano Lett., 2007, 7: 3253
23. Q. Yan, B. Huang, J. Yu, F. Zheng, J. Zhang, J. Wu, B. L. Gu, F. Liu, and W. Duan, Nano Lett., 2007, 7: 1469
24. X. Liang, Z. Fu, and S. Y. Chou, Nano Lett., 2007, 7: 3840
25. I. Meric, M. Y. Han, A. F. Young, B. Ozyilmaz, P. Kim, and K. L. Shepard, Nature Nanotechnology, 2008, 3: 654
26. X. Wu, M. Sprinkle, X. Li, F. Ming, C. Berger, and Walt A. de Heer, Phys. Rev. Lett., 2008, 101: 026801
27. J. R. Williams, L. DiCarlo, and C. M. Marcus, Science, 2007, 317: 638
28. D. A. Abanin and L. S. Levitov, Science, 2007, 317: 641
29. B. Öyilmaz, P. Jarillo-Herrero, D. Efetov, D. A. Abanin, L. S. Levitov, and P. Kim, Phys. Rev. Lett., 2007, 99: 166804
30. R. V. Gorbachev, A. S. Mayorov, A. K. Savchenko, D. W. Horsell, and F. Guinea, Nano Lett., 2008, 8: 1995
31. F. Schedin, A. K. Geim, S. V. Morozov, E. W. Hill, P. Blake, M. I. Katsnelson, and K. S. Novoselov, Nature Mater., 2007, 6: 652
32. T. O. Wehling, K. S. Novoselov, S. V. Morozov, E. E. Vdovin, M. I. Katsnelson, A. K. Geim, and A. I. Lichtenstein, Nano Lett., 2008, 8: 173
33. J. T. Robinson, F. K. Perkins, E. S. Snow, Z. Wei, and P. E. Sheehan, Nano Lett., 2008, 8: 3137
34. M. I. Katsnelson, Mater. Today, 2007, 10: 20
35. A. K. Geim and K. S. Novoselov, Nature Mater., 2007, 6: 183
36. C. W. J. Beenakker, Rev. Mod. Phys., 2008, 80: 1337
37. A. H. Castro Neto, F. Guinea, N. M. R. Peres, K. S. Novoselov, and A. K. Geim, Rev. Mod. Phys., 2009, 81: 109
38. M. Y. Han, B. Öyilmaz, Y. Zhang, and P. Kim, Phys. Rev. Lett., 2007, 98: 206805
39. Z. Chen, Y. M. Lin, M. J. Rooks, and P. Avouris, Physica E, 2007, 40: 228
40. L. Tapasztó, G. Dobrik, P. Lambin, and L. P. Biró, Nature Nanotechnology, 2008, 3: 397
41. L. Weng, L. Zhang, Y. P. Chen, and L. P. Rokhinson, Appl. Phys. Lett., 2008, 93: 093107
42. A. J. M. Giesbers, U. Zeitler, S. Neubeck, F. Freitag, K.S. Novoselov, and J. C. Maan, Solid St. Comm., 2008, 147: 366
43. X. Li, X. Wang, L. Zhang, S. Lee, and H. Dai, Science, 2008, 319: 1229
44. S. S. Datta, D. R. Strachan, S. M. Khamis, and A. T. Charlie Johnson, Nano Lett., 2008, 8: 1912
45. H. Duan, E. Xie, L. Han, and Z. Xu, Adv. Mater., 2008, 20: 3284
46. Y. Kobayashi,1, K. Fukui, T. Enoki, K. Kusakabe, and Y. Kaburagi, Phys. Rev. B, 2005, 71: 193406
47. Y. Niimi, T. Matsui, H. Kambara, K. Tagami, M. Tsukada, and H. Fukuyama, Phys. Rev. B, 2006, 73: 085421
48. Z. Liu, K. Suenaga, Peter J. F. Harris, and S. Iijima, Phys. Rev. Lett., 2009, 102: 015501
49. K. Nakada, M. Fujita, G. Dresselhaus, and M. S. Dresselhaus, Phys. Rev. B, 1996, 54: 17954
50. K. Wakabayashi, M. Fujita, H. Ajiki, and M. Sigris, Phys. Rev. B, 1999, 59: 8271
51. Y. Miyamoto, K. Nakada, and M. Fujita, Phys. Rev. B, 1999, 59: 9858
52. Y. W. Son, M. L. Cohen, and S. G. Louie, Phys. Rev. Lett., 2006, 97: 216803
53. V. Barone, O. Hod, and G. E. Scuseria, Nano Lett., 2006, 6: 2748.
54. D. Gunlycke and C. T. White, Phys. Rev. B, 2008, 77: 115116
55. X. Wang, Y. Ouyang, X. Li, H. Wang, and H. Dai, Phys. Rev. Lett., 2008, 100: 206803
56. L. Brey and H. A. Fertig, Phys. Rev. B, 2006, 73: 235411
57. Y. W. Son, M. L. Cohen, and S. G. Louie, Nature (London), 2006, 444: 347
58. L. Yang, C. H. Park, Y. W. Son, M. L. Cohen, and S. G. Louie, Phys. Rev. Lett., 2007, 99: 186801
59. B. Huang, F. Liu, J. Wu, B. L. Gu, and W. Duan, Phys. Rev. B, 2008, 77: 153411
60. E. J. Kan, Z. Li, J. Yang, and J. G. Hou, Appl. Phys. Lett., 2007, 91: 243116
61. E. Rudberg, P. Sałek, and Y. Luo, Nano Lett., 2007, 7: 2211
62. O. Hod, V. Barone, J. E. Peralta, and G. E. Scuseria, Nano Lett., 2007, 7: 2295
63. E. J. Kan, Z. Li, J. Yang, and J. G. Hou, J. Am. Chem. Soc., 2008, 130: 4224
64. F. Cervantes-Sodi, G. Csányi, S. Piscanec, and A. C. Ferrari, Phys. Rev. B, 2008, 77: 165427
65. S. Dutta and S. K. Pati, J. Phys. Chem. B, 2008, 112: 1333
66. Z. Li, H. Qian, J. Wu, B. L. Gu, and W. Duan, Phys. Rev. Lett., 2008, 100: 206802
67. A. R. Akhmerov, J. H. Bardarson, A. Rycerz, and C. W. J. Beenakker, Phys. Rev. B, 2008, 77: 205416
68. A. Cresti, G. Grosso, and G. Pastori Parravicini, Phys. Rev. B, 2008, 77: 233402
69. J. Nakabayashi, D. Yamamoto, and S. Kurihara, Phys. Rev. Lett., 2009, 102: 066803
70. W. Y. Kim and K. S. Kim, Nature Nanotechnology, 2008, 3: 408
71. K. S. Novoselov, E. McCann, S. V. Morozov, V. I. Falko, M. I. Katsnelson, U. Zeitler, D. Jiang, F. Schedin, and A. K. Geim, Nature Phys., 2006, 2: 177
72. T. Ohta, A. Bostwick, T. Seyller, K. Horn, and E. Rotenberg, Science, 2006, 313: 951
73. E. V. Castro, K. S. Novoselov, S. V. Morozov, N. M. R. Peres, J. M. B. Lopes dos Santos, J. Nilsson, F. Guinea, A. K. Geim, and A. H. Castro Neto, Phys. Rev. Lett., 2007, 99: 216802
74. M. I. Katsnelson, K. S. Novoselov, and A. K. Geim, Nat.

Phys., 2006, 2: 620
75. K. T. Lam and G. Liang, Appl. Phys. Lett., 2008, 92: 223106
76. E. V. Castro, N. M. R. Peres, J. M. B. Lopes dos Santos, A. H. Castro Neto, and F. Guinea, Phys. Rev. Lett., 2008, 100: 026802
77. B. Sahu, H. Min, A. H. MacDonald, and S. K. Banerjee, Phys. Rev. B, 2008, 78: 045404
78. D. A. Areshkin, D. Gunlycke, and C. T. White, Nano Lett., 2007, 7: 204
79. D. Gunlycke, D. A. Areshkin, and C. T. White, Appl. Phys. Lett., 2007, 90: 12104
80. D. Querlioz, Y. Apertet, A. Valentin, K. Huet, A. Bournel, S. Galdin-Retailleau, and P. Dollfus, Appl. Phys. Lett., 2008, 92: 042108
81. T. C. Li and S. P. Lu, Phys. Rev. B, 2008, 77: 085408
82. A. Lherbier, B. Biel, Y. M. Niquet, and S. Roche, Phys. Rev. Lett., 2008, 100: 036803
83. A. Cresti, N. Nemec, B. Biel, G. Niebler, F. Triozon, G. Cuniberti, and S. Roche, Nano Res., 2008, 1: 361
84. M. Evaldsson, I. V. Zozoulenko, H. Xu, and T. Heinzel, Phys. Rev. B, 2008, 78: 161407
85. E. R. Mucciolo, A. H. Castro Neto, and C. H. Lewenkopf, Phys. Rev. B, 2009, 79: 075407
86. F. Sols, F. Guinea, and A. H. Castro Neto, Phys. Rev. Lett., 2007, 99: 166803
87. C. Stampfer, J. Güttinger, F. Molitor, D. Graf, T. Ihn, and K. Ensslin, Appl. Phys. Lett., 2008, 92: 012102
88. C. Stampfer, J. Güttinger, S. Hellmüller, F. Molitor, K. Ensslin, and T. Ihn, Phys. Rev. Lett., 2009, 102: 056403
89. K. Todd, H. T. Chou, S. Amasha, and D. Goldhaber-Gordon, Nano Lett., 2009, 9: 416
90. M. Wimmer, I. Adagideli, S. Berber, D. Tomanek, and K. Richter, Phys. Rev. Lett., 2008, 100: 177207
91. D. S. Novikov, Phys. Rev. Lett., 2007, 99: 056802
92. C. L. Kane and E. J. Mele, Phys. Rev. Lett., 1997, 78: 1932
93. Y. Ouyang, Y. Yoon, J. K. Fodor, and J. Guo, Appl. Phys. Lett., 2006, 89: 203107
94. G. Liang, N. Neophytou, M. S. Lundstrom, and D. E. Nikonov, J. Appl. Phys., 2007, 102: 054307
95. V. Ryzhii, M. Ryzhii, A. Satou, and T. Otsuji, J. Appl. Phys., 2008, 103: 094510
96. P. Avouris, Acc. Chem. Res., 2002, 35: 1026
97. A. Javey, J. Guo, D. B. Farmer, Q. Wang, D. Wang, R. G. Gordon, M. Lundstrom, and H. Dai, Nano Lett., 2004, 4: 447
98. B. Huang, Q. Yan, G. Zhou, J. Wu, B. L. Gu, W. Duan, and F. Liu, Appl. Phys. Lett., 2007, 91: 253122
99. G. Liang, N. Neophytou, M. S. Lundstrom, and D. E. Nikonov, Nano Lett., 2008, 8: 1819
100. Y. Yoon and J. Guo, Appl. Phys. Lett., 2007, 91: 073103
101. D. Basu, M. J. Gilbert, L. F. Register, S. K. Banerjee, and A. H. MacDonald, Appl. Phys. Lett., 2008, 92: 042114
102. Y. Ouyang, X. Wang, H. Dai, and J. Guo, Appl. Phys. Lett., 2008, 92: 243124
103. T. B. Martins, R. H. Miwa, A. J. R. da Silva, and A. Fazzio, Phys. Rev. Lett., 2007, 98: 196803
104. A. Rycerz, J. Tworzydło, and C. W. J. Beenakker, Nature Phys., 2007, 3: 172
105. B. Huang, Z. Li, Z. Liu, G. Zhou, S. Hao, J. Wu, B. L. Gu, and W. Duan, J. Phys. Chem. C, 2008, 112: 13442